Buscarnera, G. & Einav, I. *Géotechnique* [http://dx.doi.org/10.1680/geot.10.P.118]

The yielding of brittle unsaturated granular soils

G. BUSCARNERA* and I. EINAV†

A complete thermodynamic theory is presented that is capable of explaining the dependence of yielding on the degree of saturation in brittle granular aggregates. Historically, constitutive models represented this coupling between mechanics and hydraulics only phenomenologically, by way of the incorporation of the loading collapse curve concept. This was done both for fine-grained and granular soils, and, for the latter case, without embodying the physical connection of yielding to elasticity, as motivated by fracture mechanics. Here, this connection is captured by the breakage mechanics theory, which underpins a grain-size scaling of the mechanical part of the Helmholtz free energy potential. In addition, an explicit reliance of this potential on hydraulic measures is explored, with another grain-size scaling inspired by the capillary theory. It is shown that through homogenisation these two scaling laws motivate a total macroscopic Helmholtz free energy that, together with the breakage dissipation, captures the salient couplings between mechanics and hydraulics properties, while showing a promising agreement with experiments.

KEYWORDS: gravels; partial saturation; particle crushing/crushability; theoretical analysis

Cette communication présente une théorie thermodynamique complète, permettant d'expliquer la façon dont l'affaissement est tributaire du degré de saturation dans les agrégats granulaires friables. Traditionnellement, les modèles constitutifs ne représentaient cet accouplement des facteurs mécaniques et hydrauliques que sous un plan phénoménologique, à travers l'incorporation du concept de la courbe d'affaissement sous une charge. Ces représentations portaient tant sur des sols à grain fin que sur des sols granulaires, et, dans ce dernier cas, sans incorporer le rapport physique de l'affaissement avec l'élasticité, comme étant motivé par la mécanique des fractures. Dans cette communication, ce rapport est soulevé dans le cadre de la théorie de la mécanique des ruptures, qui est à la base d'une mise à l'échelle granulométrique de la composante mécanique du potentiel d'énergie libre de Helmholtz. On se penche également sur la dépendance explicite de ce potentiel de mesures hydrauliques, ainsi que sur une autre mise à l'échelle granulométrique inspirée par la théorie capillaire. On y démontre que, par le biais de l'homogénéisation, ces deux lois dimensionnelles déterminent une énergie libre macroscopique totale de Helmholtz qui, conjointement avec la dissipation de la rupture, établit les rapports notoires existant entre les propriétés mécaniques et hydrauliques, et démontre un accord prometteur avec les expériences.

INTRODUCTION

The marked dependence of the mechanical response of soils on suction and saturation index is now well acknowledged (Alonso *et al.*, 1987; Fredlund & Rahardjo, 1993; Gens, 2010), and is forming the cornerstone of the first pioneering constitutive theories in the field of unsaturated soil mechanics (Alonso *et al.*, 1990; Wheeler & Sivakumar, 1995). Since then, a variety of different frameworks have been proposed (Jommi & di Prisco, 1994; Bolzon *et al.*, 1996; Loret & Khalili, 2002). At present, many of the constitutive models based on these frameworks tend to inherit the concepts initially developed for saturated soils, while adjusting assumptions for partially saturated conditions are used to reproduce the behavioural properties that depart from the ideal saturated case. In particular, the introduction of variables such as suction and degree of saturation proved to be a convenient basis for developing extended approaches (Gens *et al.*, 2006; Nuth & Laloui, 2008). With that in mind, it was convenient to explore the coupling between hydraulics and mechanics (Gallipoli *et al.*, 2003; Wheeler *et al.*, 2003; Sun *et al.*, 2007; Buscarnera & Nova, 2009) and the related effects of suction and degree of saturation on some key constitutive parameters (e.g. stiffness, shearing resistance, volumetric compressibility, retention properties).

One of the most important achievements has been provided by the work of Alonso *et al.* (1990). Their modelling approach made it possible to reproduce several phenomena which were at that time rather unclear (above all, the so-called wetting-collapse phenomenon). A central concept underlying their work is the idea of the loading collapse curve: that is, the notion of yield surface dependence on hydraulic variables such as suction. According to this novel idea, the yield surface can either expand or shrink upon drying or wetting respectively. Yielding can then be achieved, even at a constant total state of stress, as an outcome of wetting processes. The phenomenon of wetting-induced collapse is then explained as an irreversible compaction process.

The introduction of these concepts has clearly enlightened our understanding of the behaviour of unsaturated soils. The idea of the loading collapse curve, however, was fundamentally based on observations (i.e. the evidence that the yield condition is affected by either suction or degree of saturation). It therefore does not provide an explanation for the reasons why the surface expands upon drying and contracts during wetting.

The major goal of this paper is to investigate the notion of yielding in unsaturated materials from a rather different perspective, so that an explanation for the loading collapse curve can be provided. A thermodynamical approach is adopted for this purpose, setting up a model based on fundamental physical principles. The loading collapse curve will be directly linked to the onset of irreversible macroscopic processes, and their energy balance with corresponding fluctuations in energy-storing mechanisms. At this stage, the analysis will be restricted to irreversible processes within brittle granular aggregates and their dependence on solid–

Manuscript received 9 November 2010; revised manuscript accepted 15 February 2011.
Discussion on this paper is welcomed by the editor.
* Department of Structural Engineering, Politecnico di Milano, Italy, currently Northwestern University, Evanston, IL, USA.
† School of Civil Engineering, The University of Sydney, Australia.

fluid interactions. In such soil systems, the phenomenon of particle crushing is central, as confirmed by recent studies on unsaturated granular rockfill (Oldecop & Alonso, 2001, 2003).

Two simple, yet critical scaling assumptions will follow, regarding contributions to the Helmholtz free energy of unsaturated soils: (a) the mechanical specific strain energy contribution scales with the grain size (Einav, 2007a); and (b) the hydraulic specific energy contribution scales with the inverse of the grain size. The first assumption has proven successful to establish the physical grounds for constitutive models of brittle granular soils using the breakage mechanics theory (Einav, 2007a, 2007b), and has helped explain the physics of yielding in saturated granular materials (Einav, 2007c) and mixtures (Einav & Valdes, 2008). On the other hand, the second assumption can be justified by the capillary theory (Fisher, 1926).

In combination with homogenisation, these two grain-size-dependent scaling laws are shown to enable the deduction of a new form of macroscopic Helmholtz free energy potential for unsaturated brittle granular soils. By combining this general potential with the breakage dissipation (Einav, 2007c) a formulation will be derived that can explain how and why the mechanical yielding of brittle granular soils depends on the degree of saturation.

HYPERELASTICITY FOR UNSATURATED GRANULAR MATERIALS

This section introduces the variables describing the elastic state of unsaturated granular materials, which will be shown later to play an important role in the evolution of the inelastic variables during yielding. Analogous with fracture mechanics (Griffith, 1921; Anderson, 1995), yielding in breakage mechanics is initiated when the breakage energy, which depends on the elastic stored energy, reaches a critical value. As a result, a first key step is to clarify the thermodynamics of elasticity in unsaturated conditions.

General hyperelastic formulation

Several authors have investigated the energy input in multiphase porous media (Houlsby, 1997; Borja, 2006; Li, 2007). In the following, the energy input per unit volume will be expressed in the form obtained by Houlsby (1997) under the following assumptions: (a) incompressible solid and water phases; and (b) negligible relative movement between grains and water menisci. In addition, for the sake of simplicity, a constant atmospheric pressure will be assumed for the air phase. Even though energy statements can be devised to be more general (Coussy *et al.*, 2010; Gray *et al.*, 2010), the above-mentioned assumptions have already proven to be a reasonable starting point to enforce the first law of thermodynamics in a three-phase porous medium. The rate of work input in unsaturated soils is therefore defined as

$$\begin{aligned} W &= \left[\sigma_{ij} - u_{\mathrm{w}} S_{\mathrm{r}} \delta_{ij} - u_{\mathrm{a}}(1 - S_{\mathrm{r}})\delta_{ij}\right]\dot{\varepsilon}_{ij} - n(u_{\mathrm{a}} - u_{\mathrm{w}})\dot{S}_{\mathrm{r}} \\ &= \sigma''_{ij}\dot{\varepsilon}_{ij} - ns\dot{S}_{\mathrm{r}} \end{aligned} \tag{1}$$

where σ_{ij} is the total stress tensor, u_{w} and u_{a} are the pore water pressure and the pore air pressure respectively, δ_{ij} is the Kronecker delta, n is the soil porosity, and S_{r} is the degree of saturation.

By rearranging this expression, two stress-like variables are introduced: a generalised effective stress σ''_{ij} (having the total strain rate $\dot{\varepsilon}_{ij}$ as its associated kinematic variable); and the product ns between porosity and suction (as usual defined as $s = u_{\mathrm{a}} - u_{\mathrm{w}}$), working opposite to the rate of the saturation index ($-\dot{S}_{\mathrm{r}}$). Suction will be considered to act isotropically, thus affecting only the mean skeleton stress.

Equation (1) can in principle be reorganised in different forms, each of which implies an alternative set of work conjugate variables. In the following, σ''_{ij} will be employed as the stress measure for the solid skeleton. Even if counter-examples may be found for which such a stress measure may not be completely satisfactory (Alonso *et al.*, 2010), it is noticed that the stress variable appearing in equation (1) does in fact already provide a measure for the mean intergranular stress when the pore space is not saturated by one single fluid. It is therefore a convenient compromise to implement different sources of energy dissipation (e.g. frictional dissipation).

Let us start from the energy statement given by equation (1), and assume an isothermal, rate-independent and purely reversible hydromechanical process. In this case, the kinematic variables will be the appropriate state variables of the Helmholtz free energy. In order to define hyperelastic models for unsaturated granular materials, the first law of thermodynamics is stated as

$$W = \dot{\psi}_{\mathrm{r}} \tag{2}$$

which means that the rate of work added to the system is balanced by the rate of change of the specific Helmholtz free energy potential $\dot{\psi}_{\mathrm{r}}$. This agrees well with the concept of hyperelasticity, which implies no dissipation. The subscript r refers to a 'reference' grain size in an unbroken assembly, and its need will become clearer as the paper progresses to describe a range of grain sizes. Since in hyperelasticity the total strain is reversible, it can be seen equivalently as the elastic strain

$$\varepsilon_{ij} = \varepsilon^{\mathrm{e}}_{ij}, \text{ thus } \dot{\varepsilon}_{ij} = \dot{\varepsilon}^{\mathrm{e}}_{ij} \tag{3}$$

The previous assumptions also imply that dissipation processes related to changes in the saturation index are neglected. In this case, the saturation index is also regarded as purely reversible. In the most general case of unsaturated hyperelasticity the reference Helmholtz free energy is written in terms of those two kinematic state variables as

$$\psi_{\mathrm{r}} = \psi_{\mathrm{r}}\left(\varepsilon^{\mathrm{e}}_{ij}, S_{\mathrm{r}}\right) \tag{4}$$

where ψ_{r} is a function of the hydromechanical state variables only.

Let us specialise the above energy potential and assume that it can be decomposed into the sum of the energy stored purely mechanically (i.e. specific strain energy in the solid phase, $\psi^{\mathrm{M}}_{\mathrm{r}}(\varepsilon^{\mathrm{e}}_{ij})$) and purely hydraulically (i.e. the specific energy associated with capillary phenomena in air/water interfaces, $\psi^{\mathrm{H}}_{\mathrm{r}}(S_{\mathrm{r}})$)

$$\psi_{\mathrm{r}}\left(\varepsilon^{\mathrm{e}}_{ij}, S_{\mathrm{r}}\right) = \psi^{\mathrm{M}}_{\mathrm{r}}\left(\varepsilon^{\mathrm{e}}_{ij}\right) + \psi^{\mathrm{H}}_{\mathrm{r}}(S_{\mathrm{r}}) \tag{5}$$

The above assumption represents the simplest type of hyperelasticity for unsaturated soils, since it neglects any direct coupling between mechanical and hydraulic phenomena at the level of elastic potentials. Upon differentiation it follows that

$$\dot{\psi}_{\mathrm{r}}\left(\varepsilon^{\mathrm{e}}_{ij}, S_{\mathrm{r}}\right) = \frac{\partial \psi^{\mathrm{M}}_{\mathrm{r}}}{\partial \varepsilon^{\mathrm{e}}_{ij}}\dot{\varepsilon}^{\mathrm{e}}_{ij} + \frac{\partial \psi^{\mathrm{H}}_{\mathrm{r}}}{\partial S_{\mathrm{r}}}\dot{S}_{\mathrm{r}} \tag{6}$$

As a result, combining equations (1) and (2) and accounting for equation (6)

$$\left(\sigma''_{ij} - \frac{\partial \psi_{\mathrm{r}}^{\mathrm{M}}}{\partial \varepsilon_{ij}^{\mathrm{e}}}\right)\dot{\varepsilon}_{ij} + \left(-ns - \frac{\partial \psi_{\mathrm{r}}^{\mathrm{H}}}{\partial S_{\mathrm{r}}}\right)\dot{S}_{\mathrm{r}} = 0 \tag{7}$$

As usual, it is possible to identify the effective stress to be the conjugate of the elastic strain, while the effective suction, ns, is found to be the conjugate stress-like measure of $-S_{\mathrm{r}}$, as follows.

$$\sigma''_{ij} = \frac{\partial \psi_{\mathrm{r}}^{\mathrm{M}}}{\partial \varepsilon_{ij}^{\mathrm{e}}} \tag{8a}$$

$$ns = -\frac{\partial \psi_{\mathrm{r}}^{H}}{\partial S_{\mathrm{r}}} \tag{8b}$$

As is well known, $\psi_{\mathrm{r}}^{\mathrm{M}}$ is associated with the elastic stress–strain behaviour. Here the explicit expression of $\psi_{\mathrm{r}}^{\mathrm{H}}$ relates to the notion of 'water retention curve'. For that purpose, some possible mathematical expressions will be explored hereafter for the two functions $\psi_{\mathrm{r}}^{\mathrm{M}}$ and $\psi_{\mathrm{r}}^{\mathrm{H}}$. Given the conceptual purpose of the current paper, simplicity has been considered fundamental. Therefore the two hyperelastic functions are devised to follow the simplest possible form, which would already illustrate the promising power of the theory to reproduce qualitatively the physical phenomena concerned.

Mechanical part of the Helmholtz free energy

The Helmholtz free energy of isothermal granular materials has been investigated by many, for both linear elasticity and pressure-dependent elasticity (Houlsby, 1985; Einav & Puzrin, 2004; Houlsby *et al.*, 2005; Nguyen & Einav, 2009). The latter case clearly represents a more realistic choice to capture the Hertzian-like contact law governing the macroscopic elasticity of granular materials. However, it would be sufficient for the purpose of the initial development to assume linear isotropic hyperelasticity (here referred to a reference grain size), which could be defined as follows.

$$\psi_{\mathrm{r}}^{\mathrm{M}}\left(\varepsilon_{ij}^{\mathrm{e}}\right) = \tfrac{1}{2} K \varepsilon_{ii}^{\mathrm{e}} \varepsilon_{jj}^{\mathrm{e}} + G e_{ij}^{\mathrm{e}} e_{ij}^{\mathrm{e}} \tag{9}$$

where K and G are the effective bulk and shear moduli, while the elastic deviatoric strain is defined as $e_{ij}^{\mathrm{e}} = \varepsilon_{ij}^{\mathrm{e}} - \frac{1}{3}\delta_{ij}\varepsilon_{kk}^{\mathrm{e}}$. Then, the effective stress tensor attains the following constitutive equation

$$\sigma''_{ij} = \frac{\partial \psi_{\mathrm{r}}^{\mathrm{M}}}{\partial \varepsilon_{ij}^{\mathrm{e}}} = K \varepsilon_{kk}^{\mathrm{e}} + 2 G e_{ij}^{\mathrm{e}} \tag{10}$$

with the deviatoric stress being defined through $s_{ij} = \sigma''_{ij} - \frac{1}{3}\sigma''_{kk}\delta_{ij}$. It is then possible to isolate the isotropic and deviatoric components of the stress tensor, as follows.

$$p'' = \tfrac{1}{3}\sigma''_{kk} = K \varepsilon_{kk}^{\mathrm{e}} \text{ and } s_{ij} = 2 G e_{ij}^{\mathrm{e}} \tag{11}$$

where p'' is the mean skeleton stress.

Consulting with the outcomes of equation (1), it is worth stating that

$$\sigma''_{ij} = \sigma_{ij}^{\mathrm{net}} + s S_{\mathrm{r}} \delta_{ij} \tag{12}$$

where the net stress tensor $\sigma_{ij}^{\mathrm{net}} = \sigma_{ij} - u_{\mathrm{a}}\delta_{ij}$ has been introduced. Given the assumption that $u_{\mathrm{a}} = 0$, it is then possible to neglect this term and consider $\sigma_{ij}^{\mathrm{net}}$ as equivalent to the total stress σ_{ij}.

Hydraulic part of the Helmholtz free energy

When a molecule of water moves from the bulk volume to the interface with air, its potential energy increases (Tarantino, 2010). The outcome of such an interfacial energy is the presence of surface tension, being the major cause of capillary effects. The immediate consequence of drying processes is therefore the appearance of water menisci and the increase in the potential energy associated with capillarity.

This process must be reflected by the definition of an appropriate hydraulic contribution to the hyperelastic potential. Unlike the mechanical part of the Helmholtz free energy, which is a well-established component of thermodynamical modelling, the hydraulic part has a less straightforward meaning. For that purpose, and in order to demonstrate the eventual implications of this assumption, let us explore the following two options.

$$\psi_{\mathrm{r}}^{\mathrm{H}}(S_{\mathrm{r}}) = \tfrac{1}{2} K_{\mathrm{w}} (1 - S_{\mathrm{r}})^2 \tag{13a}$$

or

$$\psi_{\mathrm{r}}^{\mathrm{H}}(S_{\mathrm{r}}) = K_{\mathrm{w}} [S_{\mathrm{r}} - \ln(S_{\mathrm{r}}) - 1] \tag{13b}$$

where equation (13a) represents the simplest possible form for the hydraulic potential (i.e. a quadratic form, as for linear elasticity), whereas equation (13b) introduces a more realistic dependence on S_{r}. The material constant K_{w} appearing in equations (13) controls the amount of energy stored in the water menisci for a given S_{r}.

Following equation (8b), the 'effective suction' ns can be derived by differentiating $\psi_{\mathrm{r}}^{\mathrm{H}}$, as follows.

$$ns = -\frac{\partial \psi_{\mathrm{r}}^{\mathrm{H}}}{\partial S_{\mathrm{r}}} = K_{\mathrm{w}}(1 - S_{\mathrm{r}}) \tag{14a}$$

or

$$ns = -\frac{\partial \psi_{\mathrm{r}}^{\mathrm{H}}}{\partial S_{\mathrm{r}}} = K_{\mathrm{w}}\left(\frac{1}{S_{\mathrm{r}}} - 1\right) \tag{14b}$$

The above relations can be seen as two competing models for predicting the generation of suction as the material undergoes drying. They are therefore associated with the soil water retention curve (hereafter referred to as SWRC). Although the two expressions are rather different, they share the property of a zero suction $s = 0$ at the fully saturated state, $S_{\mathrm{r}} = 1$. At this state they also share the same tangent slope at $S_{\mathrm{r}} = 1$ (and hence a similar suction air entry value), determined by the same parameter

$$K_{\mathrm{w}} = -\frac{\partial (ns)}{\partial S_{\mathrm{r}}} \text{ when } S_{\mathrm{r}} = 1 \tag{15}$$

The two models gradually diverge as the saturation level reduces. When, in fact, $S_{\mathrm{r}} \to 0$, the first model predicts a finite suction of $ns = K_{\mathrm{w}}$ (i.e. in this case the interpretation for K_{w} also coincides with the intercept on the vertical axis), while the suction in the second model explodes to infinity. The simplicity of the linear assumption implies that suction data higher than a certain threshold cannot be managed, while the hyperbolic expression enables a more realistic and flexible treatment of real data, ensuring at the same time a mathematical formulation sufficiently simple for analytical developments.

A sketch of the two simple competing relationships is plotted in Fig. 1. It is worth noting that equations (14) can be reported in the usual s–S_{r} plane provided that the porosity n is given. However, since the variation of porosity before yielding is negligible, these two representations can

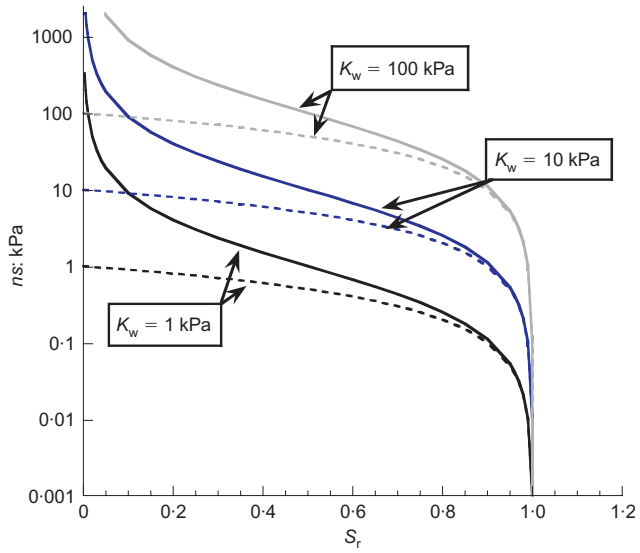

Fig. 1. Schematic plot of the two alternative water retention curves in the ns–S_r plane (dotted lines represent linear retention curve; continuous lines represent hyperbolic retention curve)

be considered equivalent for the primary purpose of this paper.

Note that both of the current SWRC models may misrepresent the effect of phenomena that become significant at high suction values (e.g. adsorption, cavitation, etc.; Frydman & Baker, 2009). Then again, simplicity has been considered critical to achieve the conceptual purpose of the current paper, which motivates continued exploration of the alternative forms given by equations (14) in the following.

ENERGY SPLIT IN UNSATURATED GRANULAR MATTER

The mechanical and hydraulic contributions to the total specific Helmholtz free energy have so far referred to a notional reference grain size. However, in order to connect the energetics of hydromechanical processes to the micromechanics of particle breakage, the effect of the grain-size distribution and its evolution must be accounted for. For that purpose two steps would follow: (a) hypotheses on how the stored energy splits between the different grain-size fractions; and (b) statistical homogenisation using the grain-size distribution as an averaging function. These two steps are at the core of the breakage mechanics theory (Einav, 2007a). In the current paper, the scaling laws governing the energy split for the hydraulic and mechanical parts of the stored energy must differ.

Let us adopt the idea that the Helmholtz free energy scales with the grain size, x. In other words, we now wish to enrich the previous description of the unsaturated hyperelasticity by adding dependence on the grain size. This assumption reflects the expectation that mechanical strain energy within the grains and hydraulic energy in interparticle menisci are stored in proportion to the grain size. This is captured by representing the specific grain-size Helmholtz free energy in the form

$$\psi\left(\varepsilon^{\mathrm{e}}_{ij}, S_{\mathrm{r}}, x\right) = \psi^{\mathrm{M}}\left(\varepsilon^{\mathrm{e}}_{ij}, x\right) + \psi^{\mathrm{H}}(S_{\mathrm{r}}, x) \tag{16}$$

Following Einav (2007a), the grain-size dependence of the mechanical part of this potential can be represented by using a multiplicative decomposition of the following form

$$\psi^{\mathrm{M}}\left(\varepsilon^{\mathrm{e}}_{ij}, x\right) = \psi^{\mathrm{M}}_{\mathrm{r}}\left(\varepsilon^{\mathrm{e}}_{ij}\right) f_{\mathrm{M}}(x) \tag{17}$$

$$f_{\mathrm{M}}(x) = \left(\frac{x}{D_{\mathrm{rM}}}\right)^{n} \tag{18}$$

where $f_{\mathrm{M}}(x)$ is the mechanical energy split function, and D_{rM} represents the mechanical reference grain size, to be defined later. We note that $f_{\mathrm{M}}(x)$ can be inspired by recognising that statistically larger particles store more strain energy (Einav, 2007a). To a first order, in the case of spherical particles, this scaling will attain quadratic dependence (i.e. $n = 2$).

Similarly, we may adopt the multiplicative decomposition to represent the scaling of the hydraulic energy on grain size,

$$\psi^{\mathrm{H}}(S_{\mathrm{r}}, x) = \psi^{\mathrm{H}}_{\mathrm{r}}(S_{\mathrm{r}}) f_{\mathrm{H}}(x) \tag{19}$$

$$f_{\mathrm{H}}(x) = \left(\frac{x}{D_{\mathrm{rH}}}\right)^{m} \tag{20}$$

with $f_{\mathrm{H}}(x)$ being the hydraulic energy split function and D_{rH} denoting the hydraulic reference grain size, to be defined later. The hydraulic split function $f_{\mathrm{H}}(x)$ can be defined on the basis of microscopic considerations. In an unsaturated granular material, in fact, there are additional forces generated by capillary effects. These forces can be quantified through the capillary theory (Fisher, 1926), and depend on the geometry of the contacts between solid grains and water menisci.

Considering ideal assembly of spheres and three-dimensional contacts, the geometry of water in the meniscus takes a toroidal shape. The size of the grains will affect the geometry of menisci and the value of suction s that can be derived from equilibrium (Gili & Alonso, 2002). A meniscus is subjected to a difference in the pressures exerted by air and water on its sides, arising because of the surface tension of water interfaces. Imposing static equilibrium for the water membrane, and considering a geometry characterised by two identical spheres with radius $R = 2x$, it follows that

$$s = u_{\mathrm{a}} - u_{\mathrm{w}} = \frac{\tau}{x} f(\theta) \tag{21}$$

where τ is the surface tension along the air/water interface and θ is the wetting angle of the meniscus (i.e. the angle that describes the geometry of the meniscus–grain contact). Equation (21) shows that $s \propto x^{-1}$. Therefore, since equation (8b) implies $s \propto -n^{-1}\partial\psi^{\mathrm{H}}(S_{\mathrm{r}}, x)/\partial S_{\mathrm{r}}$, it follows that also $\psi^{\mathrm{H}} \propto x^{-1}$. In other words, given the analytical form of equation (19), the scaling law for $f_{\mathrm{H}}(x)$ is characterised by a power function (equation (20)) with $m = -1$. This result refers to the particular case in which capillary effects represent the main interaction between solids and fluids. This interaction is here reproduced using a simplified geometry for the water meniscus that implies an inverse scaling of the hydraulic potential with the grain size. A more realistic description of the local hydromechanics may rely on the pore-size distribution rather than the grain-size distribution. At some extent, however, these two distributions are intimately linked. As a result, the use of the scaling law given by equation (20) can be considered to be a good starting point to explore the energetics of breakage in unsaturated materials.

BREAKAGE MECHANICS: GENERAL FORMULATION

Definition of breakage

The breakage of particles implies the evolution of the grain-size distribution (GSD). In this paper an internal variable, called breakage B, is introduced to track this evolution. Alternatives have been suggested in the past to quantify the amount of breakage in granular aggregates. A simple and effective way is to weigh this variable as an area

ratio between cumulative distributions as in Hardin (1985), or, as followed in breakage mechanics, by considering the ultimate cumulative distribution (Einav, 2007a). The current cumulative GSD is situated below the ultimate cumulative GSD, and the variable B is defined accordingly. In particular, it is convenient to define B so that it spans from $B = 0$ (unbroken material) when the current GSD coincides with the initial one, to $B = 1$ (breakage exhausted) when ultimate conditions are met (Fig. 2).

Quantitatively, B depends on the assumptions made for both the initial and the ultimate GSD (Fig. 2). Alternatively, one can use a universal initial GSD, given by the maximum grain size $F_0(x) = H(x - D_M)$, with H being the Heaviside function (Fig. 2(b)). The use of a universal GSD may have advantages to set up a theory based on variables that are reference free (e.g. Rubin, 2001).

Also, the choice of the ultimate GSD is not univocal. For the sake of convenience, it can be assumed to follow a power law function, conceptually associated with the progressive approach towards a fractal grading (Sammis *et al.*, 1986; McDowell *et al.*, 1996) and force attractors (Ben-Nun *et al.*, 2010). Fracture mechanics and the presence of long-range interaction forces require, however, the existence of a minimum grain size, D_m, to be recognised. It should further be accepted that by dealing with a pure breakage process, without enlargement, the grain size must be capped by a maximum D_M. The conditions for the cut-off of minima and maxima, plus the power law scaling suggest taking the following GSD density function (Einav, 2007a)

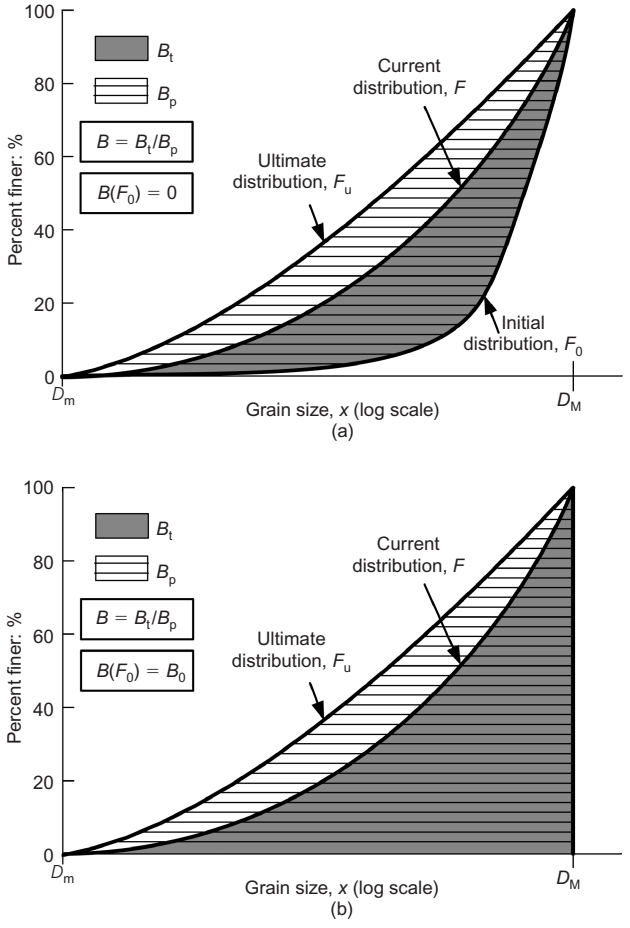

Fig. 2. Definition of breakage: (a) dependent on initial GSD; (b) universal definition as a function of D_M (see Einav, 2007a, for further discussion of the applicability of the universal definition)

$$g_u(x) = (3 - \alpha)\frac{x^{2-\alpha}}{D_M^{3-\alpha} - D_m^{3-\alpha}} \tag{22}$$

with α being the fractal dimension, typically with a value between 2·5 to 3. The quantitative definition of breakage illustrated so far enables the current GSD to be estimated as a function of B, according to

$$g(B, x) = (1 - B)\, g_0(x) + B g_u(x) \tag{23}$$

where $g(B, x)$, $g_0(x)$ and $g_u(x)$ are the current, initial and ultimate GSD. Equation (23) is based on the hypothesis of fractional independence (Einav, 2007a), which implies that the relative distance between the current, initial and ultimate density functions of any grain fractions is proportional to the distance between the corresponding cumulative distributions. Equation (23) is simplified if the universal definition for breakage is adopted, having that $g_0(x) = \delta(x - D_M)$, with δ being Dirac's delta function.

Helmholtz free energy in unsaturated breakage mechanics

Next, the Helmholtz free energy for an unsaturated porous medium is obtained by way of statistical homogenisation, where the current GSD is used to weigh the grain-size-dependent contributions, as follows.

$$\Psi\left(\varepsilon_{ij}^e, S_r, B\right) = \int_{D_m}^{D_M} g(B, x)\psi\left(\varepsilon_{ij}^e, S_r, x\right)\mathrm{d}x \tag{24}$$

The Helmholtz free energy then takes the following general form.

$$\Psi\left(\varepsilon_{ij}^e, S_r, B\right) = (1 - B)\Psi_0\left(\varepsilon_{ij}^e, S_r\right) + B\Psi_u\left(\varepsilon_{ij}^e, S_r\right) \tag{25}$$

with

$$\begin{aligned}\Psi_l\left(\varepsilon_{ij}^e, S_r\right) &= \int_{D_m}^{D_M} g_l(x)\psi\left(\varepsilon_{ij}^e, S_r, x\right)\mathrm{d}x \\ &= \int_{D_m}^{D_M} g_l(x)\left[\psi^M\left(\varepsilon_{ij}^e, x\right) + \psi^H(S_r, x)\right]\mathrm{d}x \\ &= \Psi_l^M\left(\varepsilon_{ij}^e\right) + \Psi_l^H(S_r)\end{aligned} \tag{26}$$

where the index $l = 0,u$ refers to the initial and ultimate grain-size distributions respectively.

Equation (26) can be further specified considering equations (17) and (19) for $\psi^M(\varepsilon_{ij}^e, x)$ and $\psi^H(S_r, x)$, and using the split energy functions in equations (18) and (20), to give

$$\begin{aligned}\Psi\left(\varepsilon_{ij}^e, S_r, B\right) = {} & \psi_r^M\left(\varepsilon_{ij}^e\right)[(1 - B)J_{M0} + BJ_{Mu}] \\ & + \psi_r^H(S_r)[(1 - B)J_{H0} + BJ_{Hu}]\end{aligned} \tag{27}$$

where the following grading moments have been introduced.

$$J_{M0} = \int_{D_m}^{D_M} g_0(x)\left(\frac{x}{D_{rM}}\right)^2 \mathrm{d}x \tag{28a}$$

$$J_{Mu} = \int_{D_m}^{D_M} g_u(x)\left(\frac{x}{D_{rM}}\right)^2 \mathrm{d}x \tag{28b}$$

$$J_{H0} = \int_{D_m}^{D_M} g_0(x)\left(\frac{x}{D_{rH}}\right)^{-1} \mathrm{d}x \tag{28c}$$

$$J_{Hu} = \int_{D_m}^{D_M} g_u(x)\left(\frac{x}{D_{rH}}\right)^{-1} \mathrm{d}x \tag{28d}$$

It is then convenient to choose the reference grain sizes for the mechanical and hydraulic energy split functions

according to the square root and the harmonic means of the initial GSD

$$D_{\mathrm{rM}} = \left[\int_{D_\mathrm{m}}^{D_\mathrm{M}} g_0(x)x^2\mathrm{d}x\right]^{1/2} \tag{29a}$$

and

$$D_{\mathrm{rH}} = \left[\int_{D_\mathrm{m}}^{D_\mathrm{M}} g_0(x)x^{-1}\mathrm{d}x\right]^{-1} \tag{29b}$$

which imposes $J_{\mathrm{M0}} = 1$ and $J_{\mathrm{H0}} = 1$. The two reference grain sizes are weighted means, with the probability weights scaled by the mechanical and hydraulic energy split functions respectively. The choice of the two reference values in equations (29) allows us to recover a simplified expression of the general Helmholtz free energy potential, as follows

$$\Psi\left(\varepsilon^{\mathrm{e}}_{ij},\, S_{\mathrm{r}},\, B\right) = (1-\vartheta_{\mathrm{M}}B)\psi^{\mathrm{M}}_{\mathrm{r}}\left(\varepsilon^{\mathrm{e}}_{ij}\right) + (1+\vartheta_{\mathrm{H}}B)\psi^{\mathrm{H}}_{\mathrm{r}}(S_{\mathrm{r}}) \tag{30}$$

with the following grading indices emerging out of the analysis.

$$\vartheta_{\mathrm{M}} = 1 - \frac{\displaystyle\int_{D_\mathrm{m}}^{D_\mathrm{M}} g_{\mathrm{u}}(x)x^2\mathrm{d}x}{\displaystyle\int_{D_\mathrm{m}}^{D_\mathrm{M}} g_0(x)x^2\mathrm{d}x} \tag{31a}$$

and

$$\vartheta_H = \frac{\displaystyle\int_{D_\mathrm{m}}^{D_\mathrm{M}} g_{\mathrm{u}}(x)x^{-1}\mathrm{d}x}{\displaystyle\int_{D_\mathrm{m}}^{D_\mathrm{M}} g_0(x)x^{-1}\mathrm{d}x} - 1 \tag{31b}$$

The quantities defined by equations (31) are two physical descriptors of the granular assembly. Their value depends on the limit grain-size distributions and the energy split functions $f_{\mathrm{M}}(x)$ and $f_{\mathrm{H}}(x)$. Given their definition, it can be proved that $0 \leqslant \vartheta_{\mathrm{M}} \leqslant 1$, while $\vartheta_{\mathrm{H}} \geqslant 0$.

Adopting the universal definition of breakage (i.e. with $g_0(x) = \delta(x - D_{\mathrm{M}})$), and an ultimate GSD given by the power law (equation (22)), the mechanical and hydraulic grading indices attain the following forms.

$$\vartheta_{\mathrm{M}} = 1 - \frac{3-\alpha}{5-\alpha}\left[\frac{1-(D_\mathrm{m}/D_\mathrm{M})^{5-\alpha}}{1-(D_\mathrm{m}/D_\mathrm{M})^{3-\alpha}}\right] \tag{32a}$$

and

$$\vartheta_{\mathrm{H}} = \frac{3-\alpha}{2-\alpha}\left[\frac{1-(D_\mathrm{m}/D_\mathrm{M})^{2-\alpha}}{1-(D_\mathrm{m}/D_\mathrm{M})^{3-\alpha}}\right] - 1 \tag{32b}$$

Breakage energy, breakage dissipation and energy balance during breakage

Dissipation can be added into the energy balance in the following way.

$$W = \dot{\Psi} + \Phi, \;\; \text{with } \Phi \geqslant 0 \tag{33}$$

where Φ is the rate of energy dissipation.

The rate of the Helmholtz free energy is given by

$$\dot{\Psi} = \frac{\partial\Psi}{\partial\varepsilon^{\mathrm{e}}_{ij}}\dot{\varepsilon}^{\mathrm{e}}_{ij} + \frac{\partial\Psi}{\partial S_{\mathrm{r}}}\dot{S}_{\mathrm{r}} + \frac{\partial\Psi}{\partial B}\dot{B} \tag{34}$$

Furthermore, let us decompose the total strain rate into elastic and inelastic/plastic terms, to give

$$\dot{\varepsilon}_{ij} = \dot{\varepsilon}^{\mathrm{e}}_{ij} + \dot{\varepsilon}^{\mathrm{p}}_{ij} \tag{35}$$

Combining the three equations above with the work input for unsaturated granular materials, it follows that

$$\Phi = -\frac{\partial\Psi}{\partial B}\dot{B} + \sigma''_{ij}\dot{\varepsilon}^{\mathrm{p}}_{ij} + \left(\sigma''_{ij} - \frac{\partial\Psi}{\partial\varepsilon^{\mathrm{e}}_{ij}}\right)\dot{\varepsilon}^{\mathrm{e}}_{ij} + \left(-ns - \frac{\partial\Psi}{\partial S_{\mathrm{r}}}\right)\dot{S}_{\mathrm{r}} \geqslant 0 \tag{36}$$

Consulting with the hyperelastic relations (equations (8)), the dissipation is therefore given by

$$\Phi = E_{\mathrm{B}}\dot{B} + \sigma''_{ij}\dot{\varepsilon}^{\mathrm{p}}_{ij} \geqslant 0 \tag{37}$$

where E_{B} (referred to as the breakage energy; Einav, 2007a) is defined as the conjugate of breakage:

$$E_{\mathrm{B}} = -\frac{\partial\Psi}{\partial B} \tag{38}$$

Concerning the expression of Φ, the rate of dissipation induced by breakage is distinguished from that arising by plasticity. In particular, it is convenient to introduce an additional constraint by restricting the rate of breakage dissipation to be purely dissipative

$$E_{\mathrm{B}}\dot{B} \geqslant 0 \tag{39a}$$

from which it follows that

$$\sigma''_{ij}\dot{\varepsilon}^{\mathrm{p}}_{ij} \geqslant 0 \tag{39b}$$

These two assumptions are a stronger condition than equation (37), but make it possible to constrain both processes to be purely dissipative. This section explores the case in which breakage is the only mode of dissipation, considering the other mode only at a later stage of the analysis. Inspecting solely the breakage dissipation, and since the processes of grain-size reduction implies $\dot{B} \geqslant 0$, it is evident that E_{B} must be non-negative when breakage takes place.

We may now define the breakage energy with respect to the Helmholtz free energy, as

$$E_{\mathrm{B}} = -\frac{\partial\Psi}{\partial B} = \Psi_0\left(\varepsilon^{\mathrm{e}}_{ij},\, S_{\mathrm{r}}\right) - \Psi_{\mathrm{u}}\left(\varepsilon^{\mathrm{e}}_{ij},\, S_{\mathrm{r}}\right) \tag{40}$$

Equation (40) discloses the physical meaning of E_{B} as the energy necessary to break the material from the initial to the ultimate grain-size distribution. Another useful physical quantity is the residual breakage energy, given by

$$E^*_{\mathrm{B}} = (1-B)E_{\mathrm{B}} = \Psi\left(\varepsilon^{\mathrm{e}}_{ij},\, S_{\mathrm{r}}\right) - \Psi_{\mathrm{u}}\left(\varepsilon^{\mathrm{e}}_{ij},\, S_{\mathrm{r}}\right) \tag{41}$$

which represents the energy still available to cause breakage.

These definitions are consistent with Einav (2007a, 2007c), but in the current case with the Helmholtz free energy Ψ also depending on the saturation index S_{r}. The graphical and physical interpretation of E_{B}, E^*_{B} and the breakage dissipation retains exactly the same meaning as in the dry and fully saturated cases. It can then be postulated that during breakage the variation of E^*_{B} is entirely dissipated for increasing B, and thus leading to the change of the GSD. This physical postulate can be interpreted graphically as illustrated in Fig. 3.

In mathematical terms, the incremental energy statement illustrated in Fig. 3 takes the following form

$$E_B \dot{B} = \dot{E}_B^* \tag{42}$$

Integrating the above, with $E_B^* = (1 - B)E_B$, the breakage yield condition can be defined by

$$y_B = \frac{E_B}{E_c}(1 - B)^2 - 1 \leqslant 0 \tag{43}$$

in which E_c, the critical breakage energy, is a constant of integration (Einav, 2007c).

THE HYDROMECHANICS OF BREAKAGE

Breakage under isotropic stress conditions

The consequences of having two different forms of energy stored in grains and water menisci become apparent when the breakage yield condition given by equation (43) is further explored. Let us consider at this stage only the isotropic expression of the Helmholtz energy potential, given by

$$\Psi = (1 - \vartheta_M B)\tfrac{1}{2} K \varepsilon_v^{e2} + (1 + \vartheta_H B)\psi_r^H(S_r) \tag{44}$$

where equation (9) has been reduced to its isotropic form. Equation (44) may take different expressions depending on the choices made for ψ_r^H and the related SWRC. The two alternatives given by equations (14) will be explored in the following.

Using equation (38), the breakage energy is given by

$$\begin{aligned} E_B &= -\frac{\partial \Psi}{\partial B} = \vartheta_M \psi_r^M - \vartheta_H \psi_r^H \\ &= \tfrac{1}{2}\vartheta_M K \varepsilon_v^{e2} - \vartheta_H \psi_r^H \end{aligned} \tag{45}$$

Breakage takes place when the yield condition (equation (43)) is satisfied: that is, when

$$E_B = \frac{E_c}{(1 - B)^2} \tag{46}$$

Introducing equation (45) into equation (46), and bearing in mind that $p'' = (1 - \vartheta_M B)K\varepsilon_v^e$, it is obtained that the mean effective stress at the onset of grain breakage in an unsaturated cohesionless soil is given by

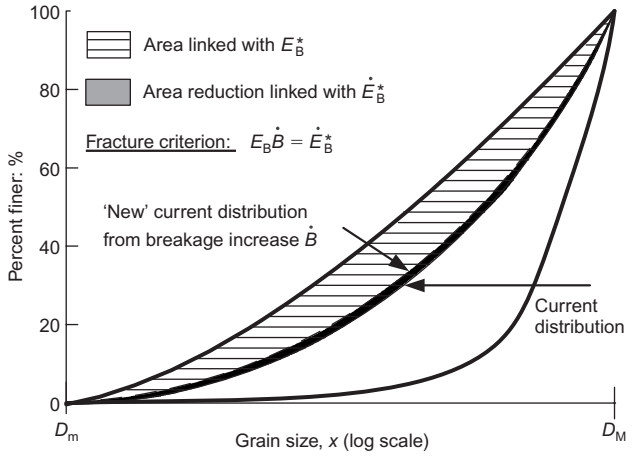

Fig. 3. Graphical interpretation of energetics of particle breakage: incremental breakage dissipation is equal to incremental change in residual breakage energy (Einav, 2007c). Similar interpretation follows when breakage is defined using the universal GSD (i.e. in alteration according to Fig. 2(b))

$$\begin{aligned} p''_{CR} &= \left(\frac{1 - \vartheta_M B}{1 - B}\right)\sqrt{\frac{2KE_C}{\vartheta_M}}\sqrt{1 + \vartheta_H \frac{\psi_r^H(S_r)}{E_c}(1 - B)^2} \\ &= p''_{CR_{SAT}} \chi_{HB}(S_r, B) \end{aligned} \tag{47}$$

in which $p''_{CR_{SAT}}$ is the comminution pressure (i.e. the pressure at the onset of breakage) for fully saturated conditions, given by

$$p''_{CR_{SAT}} = \left(\frac{1 - \vartheta_M B}{1 - B}\right)\sqrt{\frac{2KE_c}{\vartheta_M}} \tag{48}$$

while $\chi_{HB}(S_r, B)$ is given by

$$\chi_{HB}(S_r, B) = \sqrt{1 + \vartheta_H \frac{\psi_r^H(S_r)}{E_c}(1 - B^2)} \tag{49}$$

where $\psi_r^H(S_r)$ can be given either by equation (14a) or by equation (14b).

The term $\chi_{HB}(S_r, B)$ in equation (47) is a factor representing the capillary contribution to the yield stress. In the following, this factor will be referred to as hydraulic breakage factor. This coefficient describes the change in breakage yield stress with the saturation index for a brittle granular material. The influence of capillary effects on the comminution pressure threshold depends on the state variables S_r and B. The expression of the hydraulic energy potential, however, enables the conversion to the more usual representation in terms of suction. A key role is also played by the material constants ϑ_H and E_c appearing in equation (49), and by K_w (appearing in both equation (14a) and equation (14b)). In particular, a non-dimensional number can be identified, which is the main factor producing an increase in the breakage threshold with suction. This factor, here referred to as the capillary toughness number, is expressed as

$$\xi_{CT} = \vartheta_H \frac{K_w}{E_c} \tag{50}$$

The above formulation reproduces the same notion as that reflected by the so-called loading collapse curve (Alonso *et al.*, 1990) and by any other kind of phenomenological dependence of the yield domain on hydraulic state variables (Jommi & di Prisco, 1994; Gallipoli *et al.*, 2003). As long as particle breakage is not taking place, the pseudo-hardening induced by suction is a reversible hydraulic effect (in analogy with earlier models). At variance with previous formulations, however, a theoretical justification for this dependence is here provided, which can be used to predict and explain the expansion/contraction of the yield limit upon drying/wetting processes. Fig. 4 illustrates the pseudo-hardening effect induced by partially saturated conditions for different values of capillary toughness number ξ_{CT}, and for the two competing retention curves considered in the previous sections.

Higher values of ξ_{CT} imply a larger expansion of the yield limit under isotropic conditions. From equation (50) it is readily evident that a higher strength of the particles (i.e. a larger value for E_c) implies a lower increase in crushing strength with drying. Conversely, a higher suction air entry value (i.e. a larger value for K_w) implies the opposite effect on χ_{HB}. Fig. 4 shows that the SWRC also affects the predicted yield condition. This result establishes for the first time a theoretical link between the retention behaviour and the loading collapse curve. This link results from the connection between the hydromechanical energy potentials and yield, in analogy with the relation that exists between elastic energy and initiation of fracture (Griffith, 1921). In

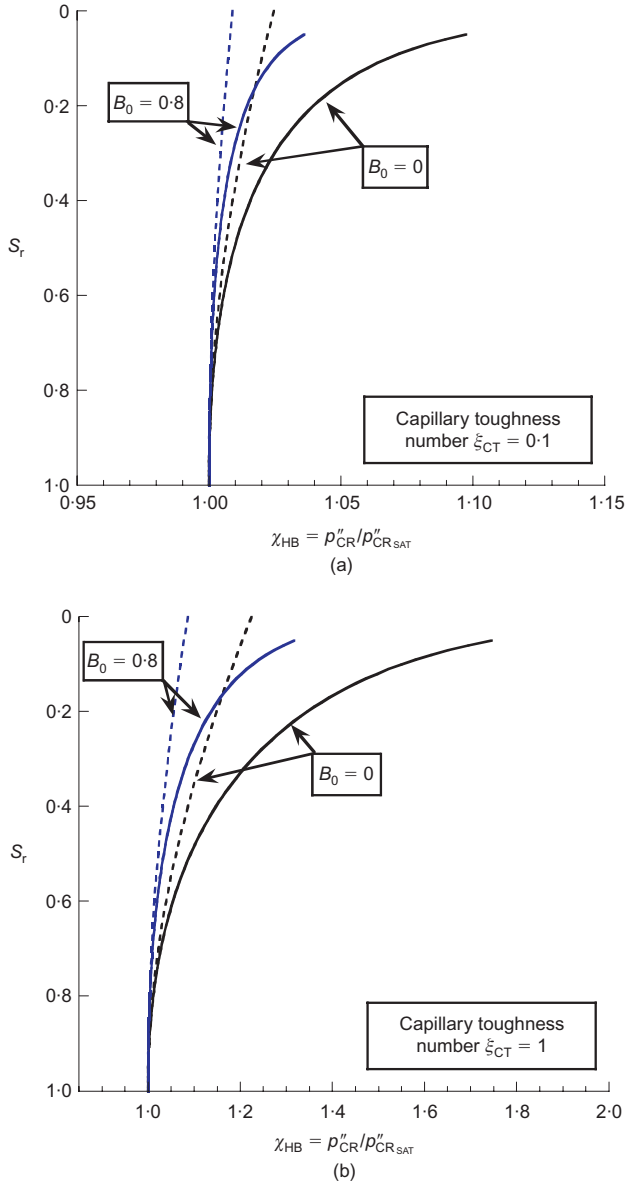

Fig. 4. Description of increase in isotropic yield limit with partial saturation: (a) $\xi_{CT} = 0{\cdot}1$; (b) $\xi_{CT} = 1$ (dotted lines represent linear retention curve; continuous lines represent hyperbolic retention curve)

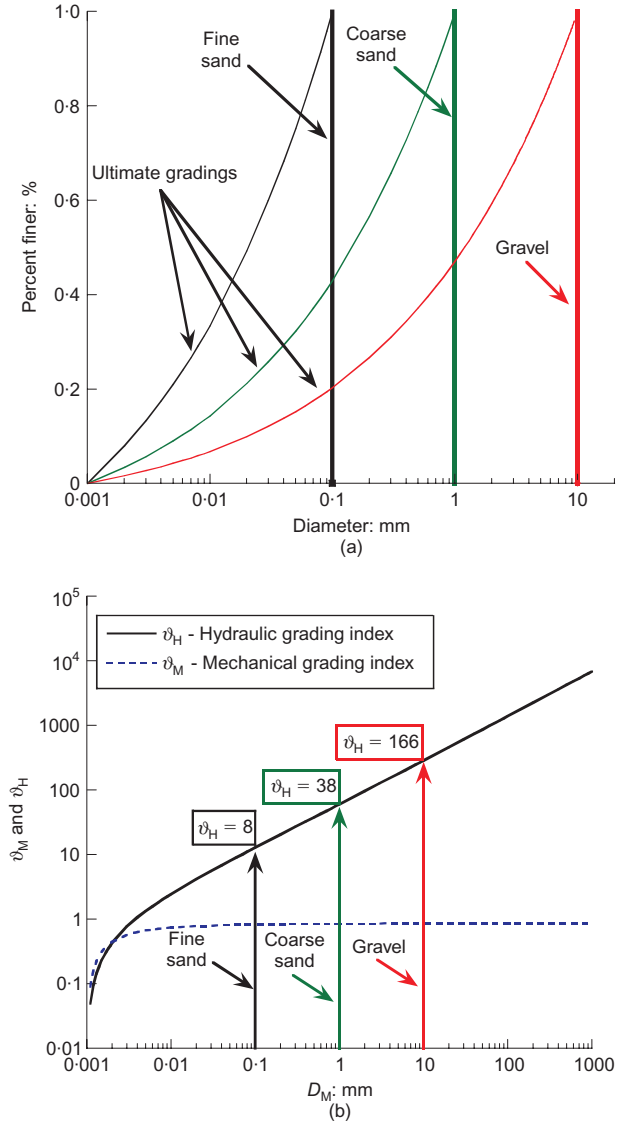

Fig. 5. (a) Examples of initial and ultimate grading curves for different granular materials; (b) dependence of ϑ_M and ϑ_H on maximum grain size for uniform initial GSD

particular, the linear retention curve predicts a finite amount of pseudo-hardening, while the latter explodes at high suction if the hyperbolic expression is used. This effect may be explained by the key role played at high suction by other physical phenomena (e.g. adsorption, cavitation) that are not reproduced in the present formulation.

An influence of the initial GSD on the hydraulic hardening effect is also envisaged, by way of the ϑ_H factor. The effect of the grain-size distribution on the grading indices ϑ_M and ϑ_H is shown in Fig. 5 as a function of the maximum grain size D_M. For this purpose, three different uniform granular materials have been considered, assuming a fractal dimension $\alpha = 2{\cdot}7$ for the ultimate GSD (the values of ϑ_M and ϑ_H have been estimated from equations (32)). Fig. 5(b) illustrates the variation of the two grading indices with D_M, having assumed a minimum value $D_m = 0{\cdot}001$ mm. While ϑ_M changes slightly with the grading, a marked effect on D_M is instead found for ϑ_H. As a result, the coefficient ξ_{CT} implicitly introduces a size dependence on the crushing strength of unsaturated granular materials, pointing out that the solid–fluid physical interaction can play a remarkable role in granular assemblies constituted by quite large particles (e.g. rockfill particles).

The result given by equation (49) indicates that χ_{HB} evolves as long as breakage proceeds. The quantitative effects of capillarity on the breakage threshold tend, in fact, to become less significant at higher values of B (Fig. 4). Thus an increase in B at constant degree of saturation has two consequences: (a) it leads to an increase in the saturated comminution pressure $p''_{CR_{SAT}}$ (often referred to as clastic hardening; McDowell & Bolton, 1998)); and (b) it implies a reduction in the hydraulic breakage factor χ_{HB}. The change in comminution yield pressure will be characterised by these two counteracting effects, and it can either increase or decrease during breakage depending on current state of saturation and material parameters (Fig. 6).

This result derives from the energy potentials describing the hydromechanics of solid–fluid interaction and the postulate on the nature of the breakage dissipation. It is interesting to note that the increase in brittleness with suction, often observed in laboratory testing of unsaturated soils, is here recovered as the natural outcome of a thermomechanical theory.

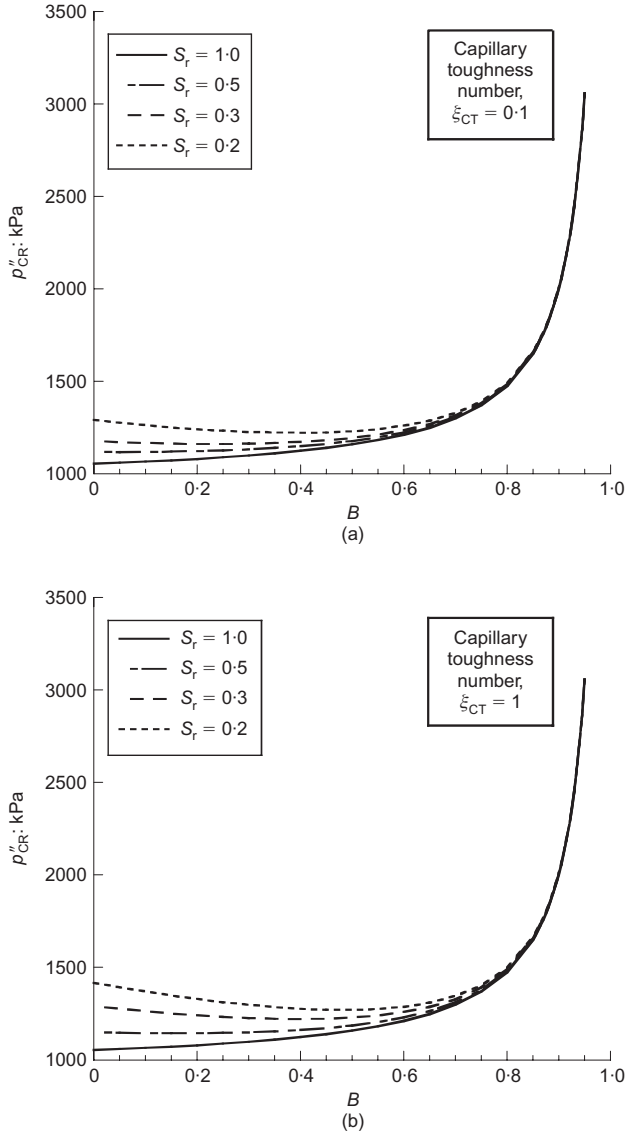

Fig. 6. Evolution of critical comminution pressure with B for different values of S_r: (a) linear retention curve; (b) hyperbolic retention curve. Figure illustrates the possibility for transition from softening to hardening for lower values of S_r

A simple model for yielding under triaxial conditions

This section extrapolates the notion of unsaturated breakage-yielding to triaxial loading conditions. This enables us to illustrate the evolution of the breakage domain with S_r, in the complete p''–q plane. For this purpose, let us adopt the yield condition (Einav, 2007c)

$$y = \frac{E_B(1-B)^2}{E_c} + \left(\frac{q}{Mp''}\right)^2 - 1 \leqslant 0 \tag{51}$$

where M is the standard frictional strength parameter for triaxial conditions. Notice that along the isotropic line (i.e. when $q = 0$) the yield criterion merges with equation (43), and its consistency condition will guarantee that the breakage evolves according to the energy balance law (equation (42)). A flow rule may be defined for the plastic shear strain rate, as in elasto-plasticity, but in breakage mechanics it further helps to define the rate of breakage

$$\dot{\varepsilon}_s^p = \lambda \frac{\partial y}{\partial q} = \lambda \frac{2q}{(Mp'')^2} \tag{52a}$$

and

$$\dot{B} = \lambda \frac{\partial y}{\partial E_B} = \lambda \frac{(1-B)^2}{E_c} \tag{52b}$$

where λ is the non-negative multiplier, as in classical elasto-plasticity. As usual, this multiplier is to be determined from the consistency condition to the yield surface in equation (51). For the sake of simplicity, the evolution of plastic volumetric strains was avoided, since it does not alter the essence of the paper (i.e. the onset of yielding and its dependence on saturation conditions). Its introduction, however, is straightforward, as illustrated by Einav (2007b,) and will be tackled in future refinements of the model.

Consulting with equation (37), it is possible to prove that the total dissipation in this model is always non-negative

$$\begin{aligned}\Phi = E_B\dot{B} + q\dot{\varepsilon}_s^p &= \lambda\left[\frac{E_B(1-B)^2}{E_c} + 2\left(\frac{q}{Mp''}\right)^2\right] \\ &= \lambda\left[1 + \left(\frac{q}{Mp''}\right)^2\right] \geqslant 0\end{aligned} \tag{53}$$

where use has been made of the yield equality in equation (51), which holds true when dissipation occurs.

In the case of a triaxial state of stress, the Helmholtz free energy function takes the form

$$\Psi = \tfrac{1}{2}(1 - \vartheta_M B)\left(K\varepsilon_v^{e2} + 3G\varepsilon_s^{e2}\right) + (1 + \vartheta_H B)\psi_r^H(S_r) \tag{54}$$

where ε_s^e is the elastic shear strain.

It is then possible to reformulate the expression for E_B in terms of the stress measures p'' and q, to give

$$E_B = -\frac{\partial \Psi}{\partial B} = \frac{\vartheta_M}{2(1-\vartheta_M B)^2}\left(\frac{p''^2}{K} + \frac{q^2}{3G}\right) - \vartheta_H \psi_r^H(S_r) \tag{55}$$

Equation (55) can now be inserted into equation (51), giving

$$\begin{aligned}&\frac{\vartheta_M}{2E_C}\left(\frac{1-B}{1-\vartheta_M B}\right)^2\left(\frac{p''^2}{K} + \frac{q^2}{3G}\right) \\ &+ \left(\frac{q}{Mp''}\right)^2 - \left(1 + \vartheta_H \frac{\psi_r^H(S_r)}{E_c}(1-B)^2\right) \leqslant 0\end{aligned} \tag{56}$$

The above expression can be further simplified by using equations (47) and (48), and introducing the quantity $r^{el} = K/3G$, as follows.

$$f_B = q \pm \frac{Mp''}{\sqrt{(p''_{CR_{SAT}})^2 + r^{el}(Mp'')^2}}\sqrt{(p''_{CR})^2 - (p'')^2} \leqslant 0 \tag{57}$$

in which f_B is the analytical form of the yield surface in the p''–q plane.

By using the above expression it is possible to have an insight into the evolution of the elastic domain with the degree of saturation, for instance during wetting processes (Fig. 7).

Besides the expansion of the elastic domain, capillary forces further imply an increase in the frictional strength, which becomes readily apparent by differentiating the yield condition $f_B(p'', q)$ above, to give

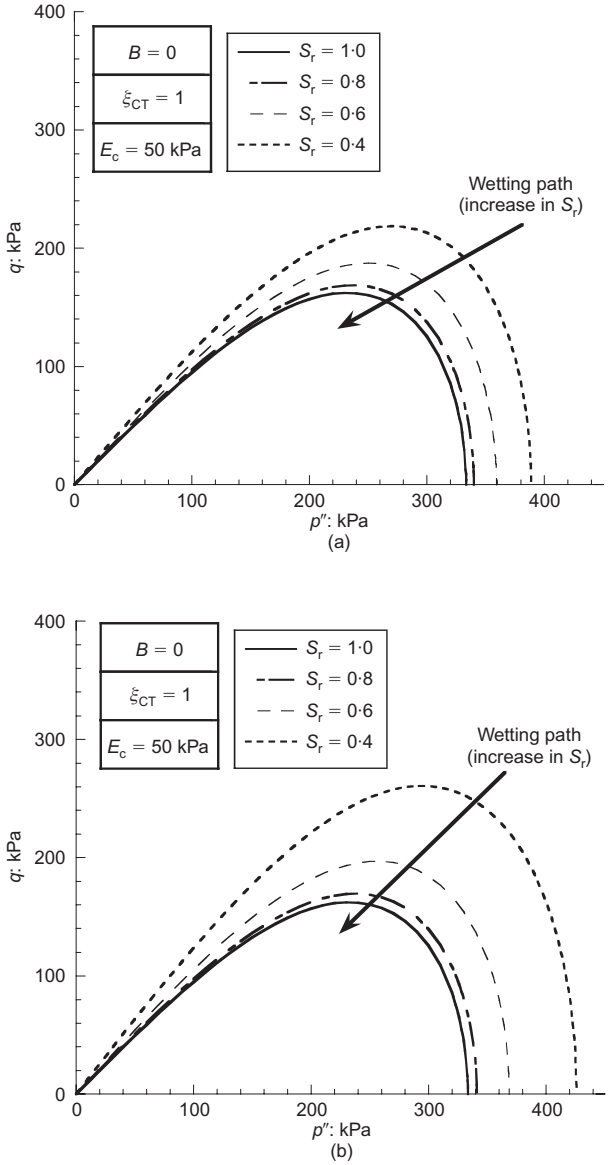

Fig. 7. Evolution of yield surface with S_r on the p''–q plane: (a) linear retention curve ($\xi_{CT} = 1$); (b) hyperbolic retention curve ($\xi_{CT} = 1$)

$$\left.\frac{\partial f_B}{\partial p''}\right|_{p''=0} = \pm M\left(\frac{p''_{CR}}{p''_{CR_{SAT}}}\right) = \pm M\chi_{HB}(S_r, B) \tag{58}$$

The increase in brittleness of the shearing response is therefore intimately linked to the increase in the predicted stress ratio at failure illustrated by equation (49).

MODELLING YIELDING IN UNSATURATED ROCKFILL

In the following the theory is evaluated against experimental data available from the literature. The selected reference material is the Pancrudo slate, a rock of Cambric origin used in the construction of the shells of a rockfill dam in Spain (Oldecop & Alonso, 2001). The mechanical behaviour of this material has been extensively explored in experimental campaigns on gravel-size granular assemblies (Fig. 8). Of particular interest for the current paper is the investigation of the effects of the saturation and wetting processes on the mechanical response (Chavez & Alonso, 2003; Oldecop & Alonso, 2003).

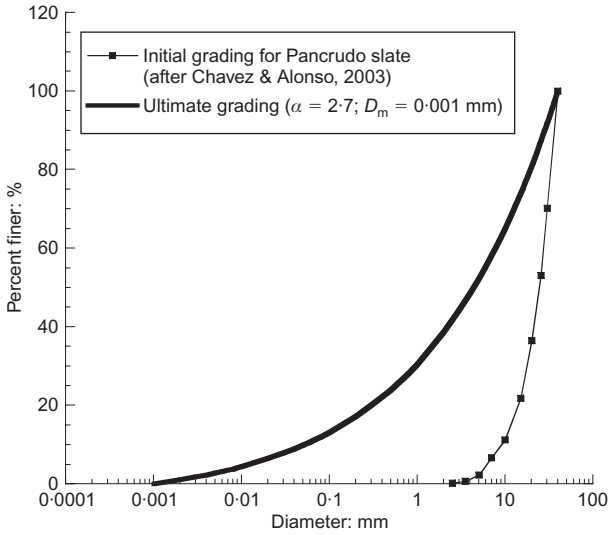

Fig. 8. Initial and ultimate grading curves for Pancrudo slate

Water retention characteristics

The theory thus far considered ideal materials, whose pore system may be adequately characterised by using only one set of macropores. Clearly, this is only an idealisation; in most cases it should be essential to accept a whole range of porosities, or at least a double-porosity hierarchical representation. In particular, the notion of double porosity seems very appealing for rockfill materials, where the two distinguishable levels of porosity may broadly represent characteristic inter- and intra-rock-particle pores. These two pore levels play different roles. For example, upon drying/wetting processes of the rockfill aggregates, it is the pores within the rock that govern the retention properties of the entire assembly, given their water storage capability. At the same time, the state of water tension within the rock pores influences the possibility of inducing particle breakage upon loading. Therefore a method is developed in the Appendix to accommodate two levels of porosity.

This method will be used to process the experimental data for Pancrudo slate. As reported by Oldecop & Alonso (2001), the assembly of Pancrudo gravelly particles is characterised by a total porosity $n = 35\%$ and a porosity of the rock units $n_m = 8\%$. According to equation (65) it follows that the porosity associated with the macropores between particles is $n_M = 30\%$. Furthermore, following equation (66), the retention properties of the entire granular rock assembly can be estimated from the water retention data available for both macropores and rock pores. The results of this data processing are shown in Fig. 9.

Given the absence of water retention data for the entire granular assembly, and considering the almost negligible retention properties of intergranular pores in gravel-like materials, a very low suction air entry value, s_{AEV}, has been considered for the macro-void space (i.e. $s_{AEV} = 0{\cdot}1$–1 Pa; Gili & Alonso, 2002). In other words, the data processing procedure assumed a negligible role of capillary effects in the intergranular region, concentrating their influence only at the pore rock scale.

The model retention curves that can capture the experiments on the Pancrudo rockfill are a slight modification of equations (14). This is done to enable a better agreement with the more complex retention behaviour, while maintaining the core of the theory. For this purpose, S_r has been replaced by an effective degree of saturation, given by

$$S_r^E = \frac{S_r - \overline{S}_r}{1 - \overline{S}_r} \tag{59}$$

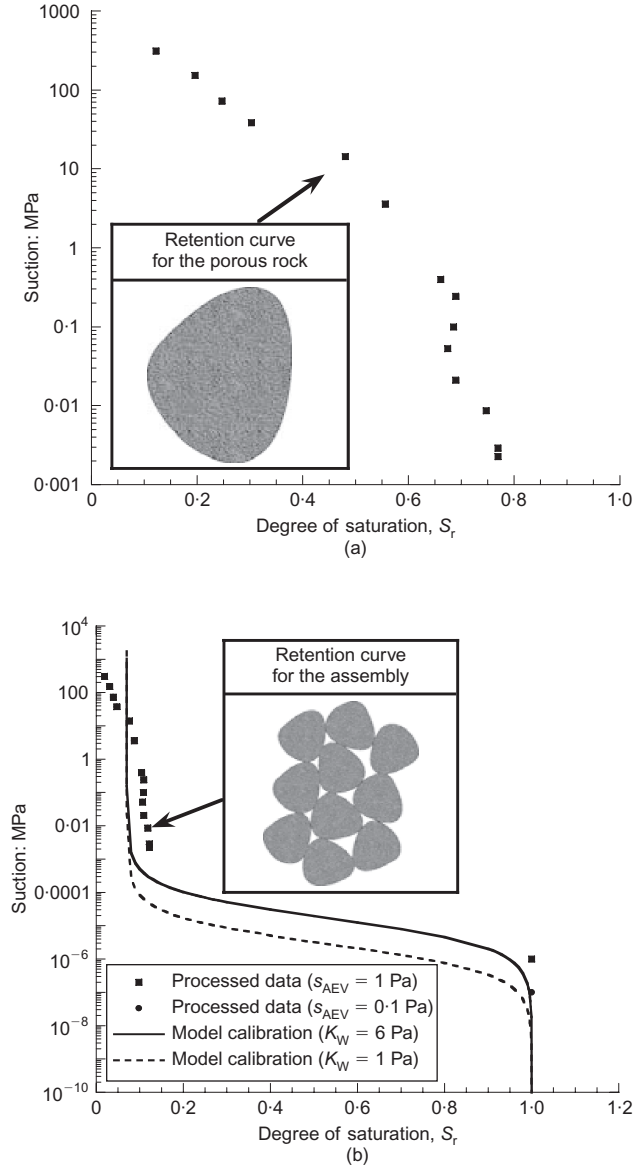

Fig. 9. (a) Water retention data for Pancrudo slate; (b) processed data and model calibration for granular assembly (residual degree of saturation $\overline{S}_r = 0{\cdot}07$; total porosity $n = 35\%$)

where the residual degree of saturation $\overline{S}_r$ has been introduced phenomenologically. This parameter reflects the presence of water tension within the grains, and provides a minimum value for S_r. Thus equations (14) become

$$ns = K_w\left(1 - \frac{S_r - \overline{S}_r}{1 - \overline{S}_r}\right) \tag{60a}$$

$$ns = K_w\left(\frac{1 - \overline{S}_r}{S_r - \overline{S}_r} - 1\right) \tag{60b}$$

being valid only for $S_r > \overline{S}_r$. From equations (60) it follows that the hydraulic energy potentials are given by

$$\psi_r^H(S_r) = \tfrac{1}{2} K_w\left(1 - \overline{S}_r\right)\left(1 - S_r^E\right)^2 \tag{61a}$$

$$\psi_r^H(S_r) = K_w\left(1 - \overline{S}_r\right)\left[S_r^E - \ln\left(S_r^E\right) - 1\right] \tag{61b}$$

This modification consistently ensures favourable improvement in prediction of the breakage onset.

Since the hydraulic potential (equation (61b)) enables us to capture the presence of high capillary tension in the rock pores, the calibration procedure will be based only on the more realistic expression (equation (60b)), as illustrated in Fig. 9(b). From the figure it is readily evident that equation (60b) guarantees improved qualitative and quantitative agreement with the data than the retention models given by equations (14) and (60a).

Yielding of unsaturated rockfill

The oedometric tests reported by Oldecop & Alonso (2003) have been reinterpreted to extract data on the onset of breakage upon loading. Fig. 10 reports some of these tests, pointing out the influence of suction on the breakage threshold.

Given the uncertainties in defining the onset of yielding from the stress–strain curves, some intervals of variation around the point of maximum curvature have been defined with error bars. The test performed at zero suction, in particular, enables the expected range of saturated critical comminution pressure to be estimated. The mechanical grading index associated with the initial GSD of the Pancrudo rockfill is $\vartheta_M = 0{\cdot}99$ (a value calculated by using $D_m = 0{\cdot}001$ mm and $\alpha = 2{\cdot}7$ in equation (22)). The hydraulic index ϑ_H has instead a value around 7·7. Assuming a value of $K_0 = \sigma'_{h0}/\sigma'_{v0} = 0{\cdot}5$, the range for the isotropic critical comminution pressure under saturated conditions is between 0·33 MPa and 0·53 MPa. The expected range of variation for E_C is obtained from equation (48), in which a value of $K = 604$ MPa has been used on the basis of the data reported by Oldecop & Alonso (2003).

The magnitude of the capillary toughness number ξ_{CT} is obtained as a function of the estimated values for E_C, K_w and ϑ_H, and ranges from 0·033 to 0·50. The hydraulic breakage factor χ_{HB} for first yielding can be calculated from equation (49), provided that the expression for $\psi_r^H(S_r)$ given by equation (61b) is used. For the case of unsaturated rockfill the critical comminution pressure, evaluated from equation (47), should be more conveniently based on a slightly modified definition for the effective pressure, p''. In fact, the microscopic features of rockfill must also be reflected by the stress measure acting on the solid skeleton. This view can be considered to be quite general for unsaturated geomaterials, as recently expounded by Alonso *et al.* (2010). In particular, the effective stress given by equation (8a) is adapted by using the effective degree of saturation, to give

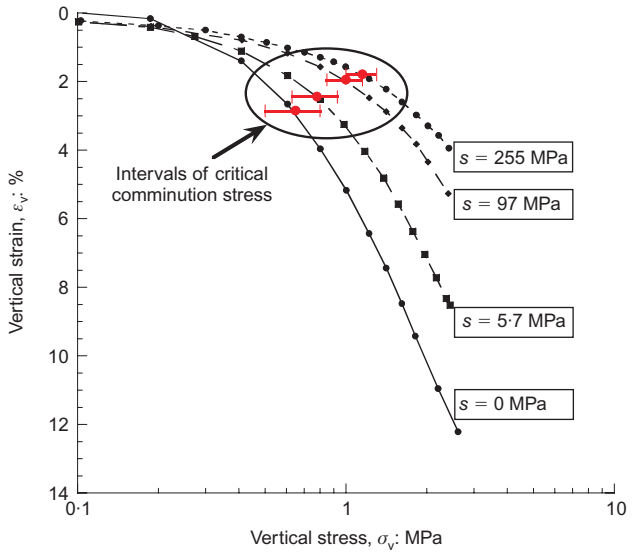

Fig. 10. Yielding upon oedometric loading: stress–strain curves (redrawn after Oldecop & Alonso, 2003)

$$p'' = p + S_r^E s = p + \frac{S_r - \overline{S}_r}{1 - \overline{S}_r} s \tag{62}$$

which is valid only for $S_r \geqslant \overline{S}_r$ and derives from the energy framework that Coussy *et al.* (2010) proposed to include the thermodynamic implications of a specific microstructure.

This assumption again reflects the distinction between the water occupying the intragranular pores and that of the pores intrinsic to the rock units. By calculating the variation of χ_{HB} with suction, a theoretical prediction for isotropic breakage stresses can be obtained. Fig. 11 shows a comparison in the suction-net isotropic stress plane between the model predictions arising from the calibration and the interpreted experimental data.

The qualitative and quantitative agreement between data and model predictions is satisfactory, given the range of uncertainty in the parameter determination. It is worth noting that the calibration has been conducted following a fully predictive approach (i.e. by estimating the fundamental constitutive parameters, namely K_w, $\overline{S}_r$, E_c and ϑ_H) separately from each other, and from the oedometric tests on unsaturated Pancrudo rockfill. The comparison shows that the theory captures the physics of breakage in partially saturated granular aggregates, enabling quantitative predictions to be made starting from first-principle considerations.

Discussion

In this section, the thermodynamics of unsaturated breakage has been applied to model the yielding of a rockfill material. This type of application is a relevant geotechnical engineering problem, where hydraulics and particle breakage interplay. The suggested thermodynamical theory was first developed for ideal systems with only a single set of macropores. However, to accommodate the evaluation for the specific case of rockfill, a comparison with the experimental data for the Pancrudo slate has been possible with some adaptations.

There are of course some remaining uncertainties related to the current analysis. First, the interpretation of phenomenological stress–strain curves to estimate yield stress data is not univocal, and it should be backed by additional observations (e.g. by acoustic emission measurements; see e.g. Fernandes *et al.*, 2010). Second, the use of the capillary theory and the associated scaling laws may be questionable at high suction values, and in the presence of water–solid interactions within the rock pores. Different physical phenomena and alternative geometrical scaling laws may then come into play in more refined analyses. Finally, the predictions presented depend on the water retention properties of the entire assembly, which were not available at this stage. Therefore assumptions have been necessary to complement the available data, as developed in the Appendix.

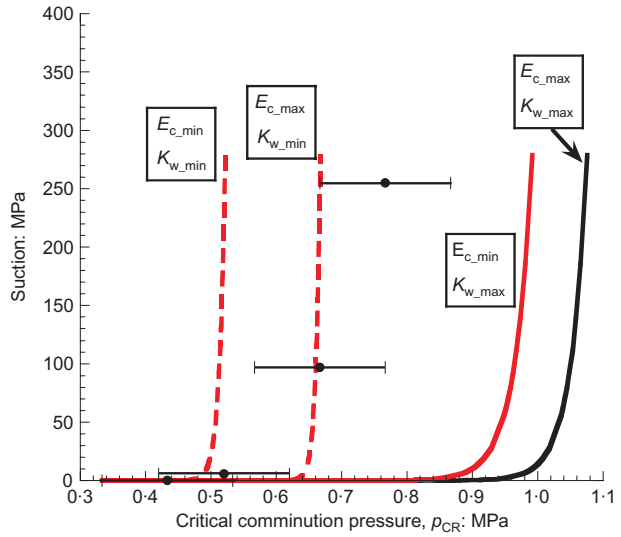

Fig. 11. Comparison of theoretical critical comminution pressures against experimental data for Pancrudo rockfill (data after Oldecop & Alonso, 2003) (error bars represent experimental data; continuous lines model predictions)

Nevertheless, the theory proves to be capable of a satisfactory qualitative and quantitative agreement with the experimental evidence. The structure of the theory is flexible enough to be adapted for the treatment of the microstructure of real soils, and the introduction of more realism into the framework (as the use of the refined retention curve, equation (60b)) significantly improves the predictive capabilities.

CONCLUSIONS

In this paper the onset of particle breakage in unsaturated granular aggregates has been investigated by extending the thermodynamic theory of breakage mechanics to unsaturated media. The theory relies on two critical ideas: (a) the assumption of particle breakage as the main source of energy dissipation at the onset of inelastic phenomena; and (b) the use of the capillary theory as the main form of solid–fluid interaction.

The paper showed that the theory of breakage mechanics can easily be extended to cope with partially saturated conditions, simply by means of energy considerations. To achieve this result, the global Helmholtz energy potential was assumed to depend not only on the usual strain energy term, but also on a hydraulic contribution associated with capillary forces. The most important distinction between these two contributions is rooted in the scaling laws governing the physics of particle interaction at the micro scale. While the specific strain energy is advocated to be stored within the particles proportional to their surface area, the specific hydraulic energy scales with the inverse of the grain size.

The implications in terms of the thermodynamics of breakage are crucial. While an increase in mechanical strain energy fosters the tendency towards reduction of the average grain size, hydraulic energy contributions counteract this possibility, favouring the survival of bigger granular aggregates. In other words, the outcome of capillary tensions is to prevent the occurrence of particle breakage, causing an increase in the energy input required to crush the material.

These notions are reflected by the breakage yield condition, and by its dependence on the saturation index. The effect of hydraulic pseudo-hardening is here naturally obtained as a system effect, starting from a microscopic hypothesis on the nature of the hydraulic energy stored within the system. The expansion/contraction of the yield limit upon drying/wetting processes and the related engineering consequences are therefore explained from an alternative perspective. The use of an energy approach discloses an unprecedented conceptual link between yielding and retention behaviour that

(*a*) allows one to reduce the number of material constants
(*b*) enables one to infer some key features of the yielding threshold from the retention behaviour (thus simplifying the calibration procedure)
(*c*) improves naturally the agreement with data if more realistic energy potentials are used (as shown through the example on unsaturated Pancrudo slate).

This result is similar to the well-known phenomenological concept of the loading collapse curve, which represents the

foundation of many constitutive frameworks aimed at describing the response of unsaturated geomaterials. At variance with previous formulations, however, the dependence on the saturation index illustrated in the current work does not arise from observation of the experimental evidence, but is naturally recovered and explained. It therefore provides a theoretical justification for the concept of the loading collapse curve, which, to the authors' knowledge, is not yet available in the literature.

As an outcome of the theory, an increase in the brittleness of the mechanical response under partially saturated conditions is also naturally reproduced, showing that microscopic solid–fluid interactions have implications for the estimate of the stress ratio at failure.

The theory developed here is based on assumptions that do not allow us to cover the entire range of unsaturated soils encountered in practice. The logic, however, can be easily exported to other systems by adding different forms of solid–fluid interaction into the formulation and improving the realism of the approach. It therefore represents a promising starting point to develop alternative modelling frameworks, and it sets a vision to shed light on different physical phenomena of practical interest.

ACKNOWLEDGEMENTS

I. E. is grateful for the support of the Australian Research Council through grant no. DP0986876, and the fund by Université Joseph Fourier to spend his study leave in Grenoble during the early half of 2010. The authors wish to acknowledge Professors Claudio di Prisco and Cino Viggiani, who arranged for the two authors of this paper to start a fruitful collaboration.

APPENDIX: WATER RETENTION OF ROCKFILL MATERIALS CONSIDERING DOUBLE POROSITY

When evaluating the theory presented in the paper against experiments, it was essential to develop an interpretation that included the notion of double porosity, relevant for rockfill materials. For that purpose, this Appendix presents a simplified procedure that makes it possible to project information from the water retention properties of a single rock unit onto those of the entire granular assembly.

The first step is to decompose the global degree of saturation, as follows.

$$S_{\mathrm{r}} = \frac{V_{\mathrm{w}}}{V_{\mathrm{v}}} = \frac{V_{\mathrm{wM}} + V_{\mathrm{wm}}}{V_{\mathrm{v}}} \tag{63}$$

where V_{wM} and V_{wm} are the volume of water contained in intergranular pores and rock pores respectively (where the subscripts 'm' and 'M' denote *m*icro and *M*acro, respectively).

Next, two local degrees of saturations may be defined for the two pore systems

$$S_{\mathrm{rM}} = \frac{V_{\mathrm{wM}}}{V_{\mathrm{vM}}} \tag{64a}$$

$$S_{\mathrm{rm}} = \frac{V_{\mathrm{wm}}}{V_{\mathrm{vm}}} \tag{64b}$$

in which V_{vM} and V_{vm} are the intergranular and rock pore volumes respectively.

When two sets of pore systems are considered, the total porosity is given by

$$\begin{aligned} n &= \frac{V_{\mathrm{v}}}{V} = \frac{V_{\mathrm{vM}} + V_{\mathrm{vm}}}{V} \\ &= n_{\mathrm{M}} + n_{\mathrm{m}}(1 - n_{\mathrm{M}}) \end{aligned} \tag{65}$$

where V is the total volume of the porous medium, n_{m} is the porosity of the rock (and hence also of the grains made of it) and n_{M} is the porosity that the material would have if the grains were non-porous. Considering equations (63)–(65), it follows that the global degree of saturation can be given by

$$S_{\mathrm{r}} = S_{\mathrm{rM}} \frac{n_{\mathrm{M}}}{n} + S_{\mathrm{rm}} \frac{n_{\mathrm{m}}(1 - n_{\mathrm{M}})}{n} \tag{66}$$

By using this equation, the retention properties of the entire granular assembly can be estimated from the water retention data available for both macropores and rock pores.

NOTATION

B	breakage internal variable
D_{rM}, D_{rH}	mechanical and hydraulic reference grain sizes
D_{m}, D_{M}	minimum and maximum grain sizes
E_{B}	breakage energy
E_{B}^{*}	residual breakage energy
E_{c}	critical breakage energy
e_{ij}^{e}	deviatoric elastic strain tensor
F	cumulative grain-size distribution function
f_{M}, f_{H}	mechanical and hydraulic energy split functions
G	elastic shear modulus
$g(B,x)$, $g_0(x)$, $g_{\mathrm{u}}(x)$	current, initial and ultimate probability densities of grain-size distribution function
K	effective bulk modulus
K_{w}	retention curve parameter
n	porosity
p	mean total stress
p''	mean generalised effective stress
p''_{CR}, $p''_{\mathrm{CR_{SAT}}}$	unsaturated and saturated comminution pressures
q	deviatoric stress
S_{r}	degree of saturation
$S_{\mathrm{r}}^{\mathrm{E}}$	effective degree of saturation
$\overline{S}_{\mathrm{r}}$	residual degree of saturation
s	suction
s_{ij}	deviatoric stress tensor
u_{a}	pore air pressure
u_{w}	pore water pressure
V	total volume of the porous medium
V_{vM}, V_{vm}	intergranular and rock pore volumes respectively
V_{wM}, V_{wm}	volume of water contained in intergranular pores and rock pores respectively
W	rate of work input per unit volume
x	grain size
y	yield function
α	fractal dimension
δ_{ij}	Kronecker delta
ε_{ij}	total strain tensor
$\varepsilon_{ij}^{\mathrm{e}}$	elastic strain tensor
$\varepsilon_{ij}^{\mathrm{p}}$	plastic strain tensor
ϑ_{M}, ϑ_{H}	mechanical and hydraulic grading indices
ξ_{CT}	capillary toughness number
σ_{ij}	total stress tensor
σ''_{ij}	generalised effective stress tensor
$\sigma_{ij}^{\mathrm{net}}$	net stress tensor
τ	surface tension into air/water interface
Φ	rate of total dissipation
χ_{HB}	hydraulic breakage factor
Ψ, Ψ^{M}, Ψ^{H}	total, mechanical and hydraulic Helmholtz free energy potentials
ψ, ψ^{M}, ψ^{H}	grain-size-dependent total, mechanical and hydraulic Helmholtz free energy potentials

REFERENCES

Alonso, E. E., Gens, A. & Hight, D. W. (1987). Special problem soils. General Report. *Proc. 9th Eur. Conf. on Soil Mech., Dublin* **3**, 1087–1146.

Alonso, E. E., Gens, A. & Josa, A. (1990). A constitutive model

for partially saturated soils. *Géotechnique* **40**, No. 3, 405–430, http://dx.doi.org/10.1680/geot.1990.40.3.405.
Alonso, E. E., Pereira, J. M., Vaunat, J. & Olivella, S. (2010). A microstructurally based effective stress for unsaturated soils. *Géotechnique* **60**, No. 12, 913–925, http://dx.doi.org/10.1680/geot.8.P.002.
Anderson, T. L. (1995). *Fracture mechanics: Fundamentals and applications*. Boca Raton, FL: CRC Press.
Ben-Nun, O., Einav, I. & Tordesillas, A. (2010). Force attractor in confined comminution of granular materials. *Phys. Rev. Lett*. **104**, No. 10, 108001.
Bolzon, G., Schrefler, B. A. & Zienkiewicz, O. C. (1996). Elasto-plastic soil constitutive laws generalized to partially saturated states. *Géotechnique* **46**, No. 2, 279–289, http://dx.doi.org/10.1680/geot.1996.46.2.279.
Borja, R. I. (2006). On the mechanical energy and effective stress in saturated and unsaturated porous continua. *Int. J. Solids Struct*. **43**, No. 6, 1764–1786.
Buscarnera, G. & Nova, R. (2009). An elastoplastic strainhardening model for soil allowing for hydraulic bonding-debonding effects. *Int. J. Numer. Anal. Methods Geomech*. **33**, No. 8, 1055–1086.
Chavez, C. & Alonso, E. E. (2003). A constitutive model for crushed granular aggregates which includes suction effects. *Soils Found*. **43**, No. 4, 215–228.
Coussy, O., Pereira, J. M. & Vaunat, J. (2010). Revisiting the thermodynamics of hardening plasticity for unsaturated soils. *Comput. Geotech*. **37**, Nos 1–2, 207–215.
Einav, I. (2007a). Breakage mechanics. Part I: Theory. *J. Mech. Phys. Solids* **55**, No. 6, 1274–1297.
Einav, I. (2007b). Breakage mechanics. Part II: Modelling granular materials. *J. Mech. Phys. Solids* **55**, No. 6, 1298–1320.
Einav, I. (2007c). Fracture propagation in brittle granular matter. *Proc. R. Soc. London Ser. A* **463**, No. 2087, 3021–3035.
Einav, I. & Puzrin, A. M. (2004). Pressure-dependent elasticity and energy conservation in elastoplastic models for soils. *J. Geotech. Geoenviron. Engng* **130**, No. 1, 81–92.
Einav, I. & Valdes, J. R. (2008). On comminution and yield in brittle granular mixtures. *J. Mech. Phys. Solids* **56**, No. 6, 2136–2148.
Fernandes, F., Syahrial, A. I. & Valdes, J. R. (2010). Monitoring the oedometric compression of sands with acoustic emissions. *ASTM Geotech. Test. J*. **33**, No. 5, GTJ102501.
Fisher, R. A. (1926). On the capillary forces in an ideal soil. *J. Agric. Sci*. **16**, 492–505.
Fredlund, D. G. & Rahardjo, H. (1993). *Soil mechanics for unsaturated soils*. New York, NY: John Wiley & Sons.
Frydman, S. & Baker, R. (2009). Theoretical soil-water characteristic curves based on adsorption, cavitation and a double porosity model. *Int. J. Geomech*. **9**, No. 6, 250–257.
Gallipoli, D., Gens, A., Sharma, R. S. & Vaunat, J. (2003). An elasto-plastic model for unsaturated soil incorporating the effect of suction and degree of saturation on mechanical behaviour. *Géotechnique* **53**, No. 2, 123–135, http://dx.doi.org/10.1680/geot.2003.53.2.123.
Gens, A. (2010). Soil–environment interactions in geotechnical engineering. *Géotechnique* **60**, No. 1, 3–74, http://dx.doi.org/10.1680/geot.9.P.109.
Gens, A., Sanchez, M. & Sheng, D. (2006). On constitutive modelling of unsaturated soils. *Acta Geotech*. **1**, No. 3, 137–147.
Gili, J. A. & Alonso, E. E. (2002). Microstructural deformation mechanisms of unsaturated granular soils. *Int. J. Numer. Anal. Methods Geomech*. **26**, No. 5, 433–468.
Gray, W. G., Schrefler, B. A. & Pesavento, F. (2010). Work input for unsaturated elastic porous media. *J. Mech. Phys. Solids* **58**, No. 5, 752–765.
Griffith, A. A. (1921). The phenomena of rupture and flow in solids. *Phil. Trans. R. Soc. London Ser. A* **221**, 163–198.
Hardin, B. O. (1985). Crushing of soil particles. *J. Geotech. Engng ASCE* **111**, No. 10, 1177–1192.
Houlsby, G. T. (1985). The use of a variable shear modulus in elastic-plastic models for clays. *Comput. Geotech*. **1**, No. 1, 3–13.
Houlsby, G. T. (1997). The work input to an unsaturated granular material. *Géotechnique* **47**, No. 1, 193–196, http://dx.doi.org/10.1680/geot.1997.47.1.193.
Houlsby, G. T., Amorosi, A. & Rojas, E. (2005). Elastic moduli of soils dependent on pressure: a hyperelastic formulation. *Géotechnique* **55**, No. 5, 383–392, http://dx.doi.org/10.1680/geot.2005.55.5.383.
Jommi, C. & di Prisco, C. (1994). Un semplice approccio teorico per la modellazione del comportamento meccanico dei terreni granulari parzialmente saturi. *Conference Il Ruolo dei Fluidi nei Problemi di Ingegneria Geotecnica*, Mondoví, pp. 167–188.
Li, X. S. (2007). Thermodynamics-based constitutive framework for unsaturated soils. 1: Theory. *Géotechnique* **57**, No. 5, 411–422, http://dx.doi.org/10.1680/geot.2007.57.5.411.
Loret, B. & Khalili, N. (2002). An effective stress elastic–plastic model for unsaturated porous media. *Mech Mater*. **34**, No. 2, 97–116.
McDowell, G. R. & Bolton, M. D. (1998). On the micromechanics of crushable aggregates. *Géotechnique* **48**, No. 5, 667–679, http://dx.doi.org/10.1680/geot.1998.48.5.667.
McDowell, G. R., Bolton, M. D. & Robertson, D. (1996). The fractal crushing of granular materials. *J. Mech. Phys. Solids* **44**, No. 12, 2079–2102.
Nguyen, G. D. & Einav, I. (2009). The energetics of cataclasis based on breakage mechanics. *Pure Appl. Geophys*. **166**, No. 10, 1693–1724.
Nuth, M. & Laloui, L. (2008). Effective stress concept in unsaturated soils: clarification and validation of a unified framework. *Int. J. Numer. Anal. Methods Geomech*. **32**, No. 7, 771–801.
Oldecop, L. & Alonso, E. E. (2001). A model for rockfill compressibility. *Géotechnique* **51**, No. 2, 127–140, http://dx.doi.org/10.1680/geot.2001.51.2.127.
Oldecop, L. A. & Alonso, E. E. (2003). Suction effects on rockfill compressibility. *Géotechnique* **53**, No. 2, 289–292, http://dx.doi.org/10.1680/geot.2003.53.2.289.
Rubin, M. B. (2001). Physical reasons for abandoning plastic deformation measures in plasticity and viscoplasticity theory. *Arch. Mech*. **53**, Nos 4–5, 519–539.
Sammis, C. G., Osborne, R. H., Anderson, J. L., Banerdt, M. & White, P. (1986). Self-similar cataclasis in the formation of fault gouge. *Pure Appl. Geophys*. **124**, No. 1, 53–78.
Sun, D., Sheng, D. & Sloan, S. (2007). Elastoplastic modelling of hydraulic and stress–strain behaviour of unsaturated soils. *Mech. Mater*. **39**, No. 3, 212–221.
Tarantino, A. (2010). Basic concepts in the mechanics and hydraulics of unsaturated geomaterials. In *Mechanics of unsaturated geomaterials* (ed. L. Laloui), pp. 3–28. Hoboken, NJ: Wiley.
Wheeler, S. J. & Sivakumar, V. (1995). An elasto-plastic critical state framework for unsaturated soils. *Géotechnique* **45**, No. 1, 35–53, http://dx.doi.org/10.1680/geot.1995.45.1.35.
Wheeler, S. J., Sharma, R. S. & Buisson, M. S. R. (2003). Coupling of hydraulic hysteresis and stress–strain behaviour in unsaturated soils. *Géotechnique* **53**, No. 1, 41–54, http://dx.doi.org/10.1680/geot.2003.53.1.41.